Am J Nucl Med Mol Imaging 2013;3(2):118-128
www.ajnmmi.us /ISSN:2160-8407/ajnmmi1210004

Original Article

Evaluation of bone remodeling with ^{18}F-fluoride and correlation with the glucose metabolism measured by ^{18}F-FDG in lumbar spine with time in an experimental nude rat model with osteoporosis using dynamic PET-CT

Caixia Cheng[1], Christian Heiss[2,3], Antonia Dimitrakopoulou-Strauss[1], P Govindarajan[3], G Schlewitz[2], Leyun Pan[1], Reinhard Schnettler[2], Klaus Weber[4], Ludwig G Strauss[1]

[1]Clinical Cooperation Unit Nuclear Medicine, German Cancer Research Center, Heidelberg, Germany; [2]Department of Trauma Surgery, University Hospital Giessen-Marburg GmbH, Giessen, Germany; [3]Laboratory of Experimental Trauma Surgery, Justus-Liebig University, Giessen, Germany; [4]Department of Radiopharmaceutical Chemistry, German Cancer Research Center, Heidelberg, Germany

Received October 29, 2012; Accepted December 18, 2012; Epub March 8, 2013; Published March 18, 2013

Abstract: Rats with osteoporosis were involved by combining ovariectomy (OVX) either with calcium and Vitamin D deficiency diet (Group D), or with glucocorticoid (dexamethasone) treatment (Group C). In the period of 1-12 months, dynamic PET-CT studies were performed in three groups of rats including Group D, Group C and the control Group K (sham-operated). Standardized uptake values (SUVs) were calculated, and a 2-tissue compartmental learning-machine model (calculation of K1-k4, VB and the plasma clearance of tracer to bone mineral (Ki) as well as a non-compartmental model based on the fractal dimension (FD) was used for quantitative analysis of both groups. The evaluation of PET data was performed over the lumbar spine. The correlation analysis revealed a significant linear correlation for certain dPET quantitative parameters and time up to 12 months after induction of osteoporosis. Based on the ^{18}F-Fluoride data, we noted a significant negative correlation for K1 (the fluoride/hydroxyl exchange) in the Group C and a significant positive correlation for k3, SUV (bone metabolism) and FD in the Group K. The evaluation of the ^{18}F-FDG data revealed a significant positive correlation for SUV (glucose metabolism) only in Group C. The correlation between the two tracers revealed significant results between K1 of ^{18}F-Fluoride and SUV of FDG in Group K as well as between FD of ^{18}F-Fluoride and FDG in Group D and C and between k3 of ^{18}F-Fluoride and SUV of FDG in Group C.

Keywords: dPET-CT, ^{18}F-FDG, ^{18}F-fluoride, osteoporosis

Introduction

Osteoporosis is an emerging medical and socioeconomic threat characterized by a systemic impairment of bone mass, strength, and micro-architecture, which increases the probability of fragility fractures [1]. Osteoporosis is more common in postmenopausal women than in men of similar age (40-50% vs. 13-22%) and expected to increase by more than 3-fold over the next 50 years [2-4]. Many fracture types are associated with osteoporosis, but hip, spine, forearm and shoulder are the most common sites [5].

To prevent the first fracture, early assessment of an individual's risk of osteoporosis is therefore important. The measurement of bone mineral density (BMD) by dual energy X-ray absorptiometry (DEXA) is a valid method to diagnose osteoporosis and to predict the risk of fracture, and has been commonly used for clinical phase-3 studies [6, 7]. In addition, advances in imaging techniques with high-resolution peripheral CT that yield volumetric bone-density data might allow better prediction of bone strength and thus fracture risk [8].

Positron emission tomography (PET) permits quantification of biochemical process in vivo

and is routinely used in neurological, cardiac and oncological applications [9, 10]. In the early 1990s, ^{18}F-FDG was evolving as a major tool in the field of oncology. FDG-PET was furthermore reported for differentiation between osteoporotic and pathological vertebral fractures [11]. Meanwhile, ^{18}F-fluoride PET introduced as a technique for quantifying bone metabolism by Hawkins et al., who first described the 3-compartmental kinetic model that can be applied in clinical studies [12]. ^{18}F- is a positron emitting radionuclide. After diffusion through bone capillaries into bone extracellular fluid, fluoride ion exchanges with hydroxyl groups in the hydroxyapatite crystal to form fluoroapatite [13]. Fluoride is preferentially deposited at the surfaces of bone where remodeling and turnover is greatest [14, 15]. Employing plasma clearance methods, this tracer has been used to measure total skeletal blood flow, which has been shown to correlate with osteoblast rate in iliac trabeculae and skeletal influx rate of calcium in osteoporotic patients [16].

The aim of current study, which is part of a large multicenter project focusing on osteoporosis, was to measure and compare regional skeletal kinetics at trabecular bone (lumbar spine) in a rat model, using ^{18}F-Fluoride and ^{18}F-FDG dynamic PET-CT (dPET-CT) in normal and osteoporosis induced rats. Osteoporosis was induced either by ovariectomy plus a restricted calcium and Vitamin D diet or by ovariectomy and steroid (dexamethasone) administration. The ^{18}F-fluoride PET data were also compared with the ^{18}F-FDG PET data regarding the changes in the FDG metabolism/kinetics in control, diet- and glucocorticoid-induced osteoporotic rats over time up to 12 months after induction of osteoporosis. Furthermore, considering the multifactorial aspects, attempts were made to draw interrelations between the different types of induction of osteoporosis and the time points after osteoporosis induction.

Materials and methods

Animal characteristics, treatment

Female Sprague Dawley rats aged 10 weeks were purchased from Charles River (Sulzfeld, Germany). The average weights of the animals were in a range between 250-290 g and were maintained under standard laboratory conditions. Animals underwent an acclimatization period of four weeks before the experimental procedures. The animals and all the experimental procedures were approved by German animal protection laws of district government ("Regierungspräsidium Giessen" RP (89/2009)).

The animals were grouped into three categories: Group K (control group, sham operated), Group D (ovariectomy and diet) and Group C (ovariectomy and steroid). Each group consisted of 8-9 rats, which have been examined over time (2-3 rats for each time point). At the age of 14 weeks from birth, the animals of Group K underwent only a surgical procedure of laparotomy (without ovariectomy) after being anaesthesized with intraperitoneal injection of 62.5 mg/kg B. wt. ketamine (Hostaket®, Hoechst) and 7.5 mg/kg B. wt. xylazine (Rompun®, Bayer) and were fed with normal feed (sham operation). Group D animals were ovariectomized and were fed two weeks post surgery with deficient diet (deficient in vitamin D2/D3, vitamin C, calcium, soy-free, phytoestrogen free and scarce phosphorus supply, purchased from Altromin (Altromin-C1034, Altromin Spezialfutter GmbH, Lage, Germany). Group C rats were ovariectomized followed by receiving glucocorticoid injection of dexamethasone-21-isonicotinate (Voren-Depot®, Boehringer Ingelheim, Germany) at a dose of 0.3 mg/kg B. wt., applied once every three weeks. The steroid administration was started postoperative two weeks after the ovariectomy of the animals.

At varied time points of 1, 3, and 12 months, dPET-CT studies were performed. During scanning, rats were anesthetized using a mixture of nitrous oxide (1 l/min), oxygen (0.5 l/min) and isoflurane (1.5 vol.%).

Radiopharmaceuticals

The preparation of ^{18}F-FDG was done according to the method described by Toorongian et al. [17]. ^{18}F-Fluoride was prepared by 11-MeV proton irradiation of [^{18}O]water in a Nb target body using a MC32Ni cyclotron. The irradiated aqueous solution containing [^{18}F]fluoride was passed through an anion exchange cartidge (Sep-Pak Accell Plus QMA; bicarbonate form) to trap the [^{18}F]fluoride. The cartridge was then eluted with sterile isotonic NaCl solution fol-

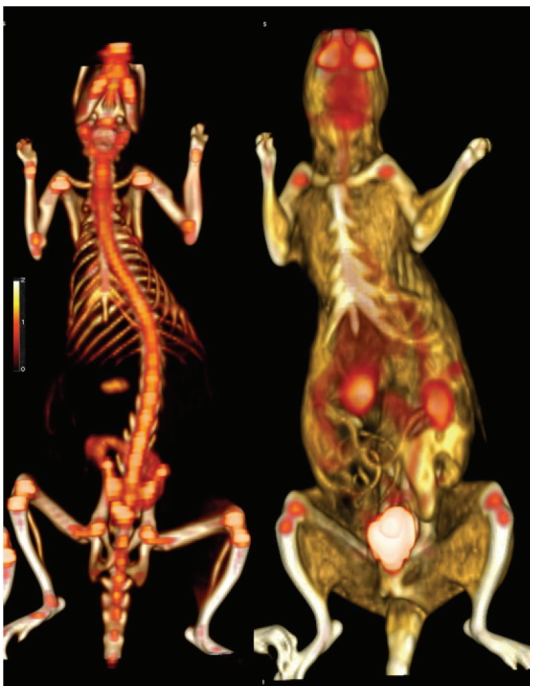

Figure 1. 3D fused PET-CT images for ^{18}F-fluoride (left) and ^{18}F-FDG (right) in two rats of Group K. The ^{18}F-fluoride image demonstrates the whole body tracer distribution in a rat and shows an enhanced uptake mainly in the bones, and joints cartilages. Furthermore, the images demonstrate an enhanced uptake in the urinary bladder and the kidneys due to the tracer excretion. The ^{18}F-FDG images demonstrate an enhanced uptake in the brain, heart, as well as in the knee and shoulder joints (unspecific uptake), but also in the kidneys and urinary bladder (due to tracer excretion).

lowed by sterile fitration. The quality control complied with the European Pharmacopoeia, as reported previously [18].

PET, kinetic model

Dynamic PET studies were performed for 60 min after the intravenous application of 20 to 40 MBq taking the changing weight of rats into account ^{18}F-fluoride or ^{18}F-FDG, using a 28-frame protocol (10 frames of 30 seconds, 5 frames of 60 seconds, 5 frames of 120 seconds, and 8 frames of 300 seconds). A dedicated PET-CT system (Biograph™ mCT, 128 S, Siemens Co, Erlangen, Germany) with an axial field of view of 21.6 cm with high resolution and TrueV, operated in a 3-dimensional mode, was used for all animal studies. The system provides the simultaneous acquisition of 369 transverse slices with a slice thickness of 0.6 mm. The animals were positioned in the axial plane of the system to maintain the best resolution in the center of the system. An ultrahigh resolution CT scan was performed prior the PET scanning with 160 mA, 80 kV, pitch of 0.85 cm for attenuation correction of the acquired dynamic emission data. All PET images were attenuation-corrected and an image matrix of 400x400 pixels was used for iterative image reconstruction (voxel size 1.565x1.565x0.6 mm) based on the syngo MI PET/CT 2009C software version. The reconstructed images were converted to standardized uptake value (SUV) images [19]. The SUV 55-60 min post-injection was used for the assessment of both tracers. The SUV images were used for all further quantitative evaluations.

Dynamic PET data were evaluated using the software package PMOD (provided courtesy of PMOD Technologies Ltd., Zuerich, Switzerland) [20, 21]. We evaluated the tracer uptake in the lumbar spine, using VOI´s and an isocontour of 50%. A volume of interest consists of several regions of interest over the target area. In the case of ^{18}F-FDG, lumbar spine was replaced by thoracic vertebrae because of its invisibility (**Figure 1**). For input we used 10 contiguous PET slices in the middle and lower third of aorta. We avoided using the upper part of the thoracic aorta due to spillover from the heart. A detailed quantitative evaluation of tracer kinetics requires the use of compartmental modeling. A 2-tissue-compartment model was used to evaluate the dynamic studies. This methodology is used primarily for scientific purposes, for the quantification of dynamic ^{18}F-FDG studies [22, 23]. The 2-tissue compartment model can also be used for the evaluation of ^{18}F-Fluoride studies [24].

A partial volume correction was not performed because the recovery coefficient was 0.8 for a diameter of 8 mm and 0.2 for a diameter of 3 mm based on phantom measurements as well as the recent parameter settings used with the reconstruction software. For the input function the mean values of the VOI data obtained from the aorta were used.

In the current study, the learning-machine two-tissue compartment model was used for the fitting and provided five parameters: the plasma clearance to the bone extracellular fluid (ECF) compartment and the rate constant for return

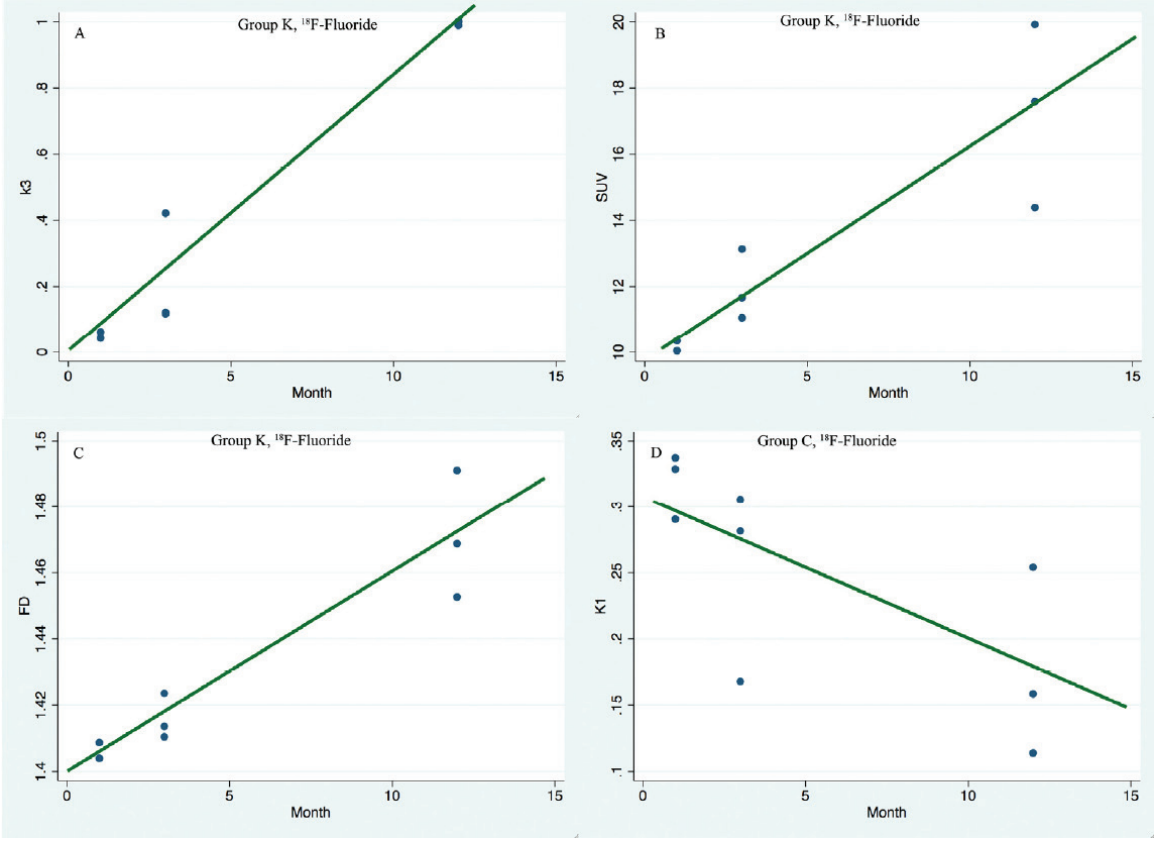

Figure 2. Scatter plots of dPET quantitative parameters and time for ^{18}F-Fluoride. A significant correlation was obtained using a linear regression fit for (A) k3 for the Group K (r=0.98, p<0.00001), (B) SUV for the Group K (r=0.89, p<0.01), (C) FD for the Group K (r=0.94, p<0.001), (D) K1 for the Group C (r=-0.72, p<0.05).

of tracer to plasma, K1 and k2, the rate constants describing movement of tracer into and out of the bound bone compartment, k3 and k4, and the fractional blood volume, also called vessel density (VB), which reflects the amount of blood in the VOI. Following compartment analysis, we calculated the plasma clearance of tracer to bone mineral from the compartment data using the formula: influx = (K1*k3)/(k2+k3). Compared to the standard iterative method, the machine learning method has the advantage of a fast convergence and avoidance of over fitting [25]. The model parameters were accepted when K1-k4 was less than 1 and VB exceeded 0. The unit for the rate constants K1-k4 was 1/min.

Besides the compartmental analysis, a non-compartmental model based on the fractal dimension was used. The fractal dimension is a parameter of heterogeneity and was calculated for the time-activity data of each individual volume of interest. The values for fractal dimension vary from 0 to 2, showing the deterministic or chaotic distribution of tracer activity. We used a subdivision of 7 X 7 and a maximal SUV of 20 for the calculation of fractal dimension [26]. More details on the methodology used were published elsewhere [24].

Statistical analysis

Statistical evaluation was performed with Stata/SE 10.1 (stataCorp, College Station, TX). Statistical evaluation was performed using the descriptive statistics, scatterplots and pairwise correlations. For the correlation analysis, a significance level of P <0.05 was used. Based on the significant results of the correlation analysis, linear regression functions were calculated for the PET data and time points.

Results

PET-CT analysis

Figure 1 demonstrates that ^{18}F-Fluoride preferentially accumulates in bone structures, while

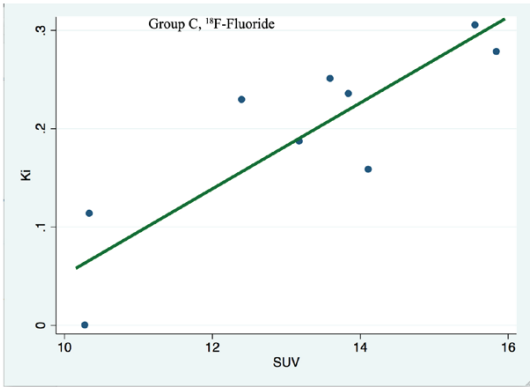

Figure 3. The Scatter plot of SUV and Ki for ^{18}F-Fluoride demonstrated a significant correlation obtained using a linear regression fit in the lumbar spine for the Group C (r=0.85, p<0.01).

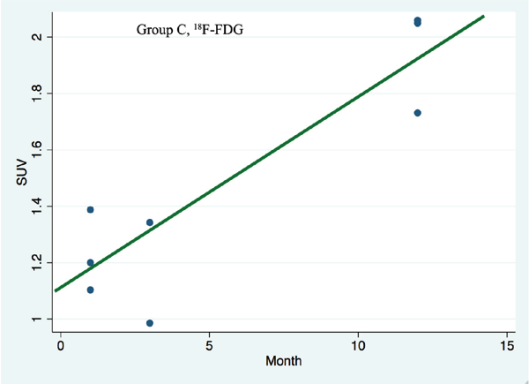

Figure 4. The Scatter plot of SUV and time for ^{18}F-FDG demonstrated a significant correlation obtained using a linear regression fit in the lumbar spine for the Group C (r=0.90, p<0.01).

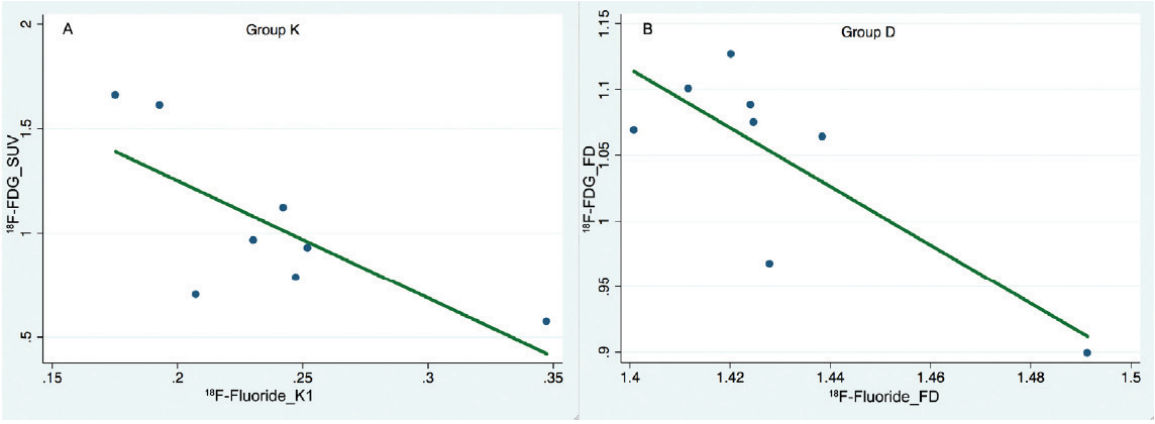

Figure 5. Scatter plots of dPET quantitative parameters from ^{18}F-Fluoride and ^{18}F-FDG. A significant correlation was obtained using a linear regression fit for (A) K1 of ^{18}F-Fluoride and SUV of ^{18}F-FDG in Group K (r=-0.73, p<0.05), (B) FD of ^{18}F-Fluoride and FD of ^{18}F-FDG in Group D (r=-0.80, p<0.05).

^{18}F-FDG reflects the glucose metabolism in tissue. There is a normal enhanced FDG uptake in the brain and liver as well as in the urinary bladder and kidneys due to the tracer excretion. ^{18}F-Fluoride accumulates primarily in the bones and joint cartilages but there may be an uptake in the kidneys and urinary bladder due to tracer excretion.

Quantitative analysis

F-18-Fluoride: We correlated the ^{18}F-Fluoride quantitative parameters within time after the induction of osteoporosis up to 12 months. The results in Group K demonstrated significant correlations between time and the parameters k3, SUV and FD on the p<0.05 level (**Figure 2A-C**). The value of r was 0.98, 0.89 and 0.94, respectively. Furthermore, the parameter k2 decreased significantly with time (data not shown).

For Group C, a significant negative correlation with p<0.05 was noted for K1 and the time (1-12 months) with r=-0.72 (linear correlation) (**Figure 2D**). In addition, a significant correlation between Ki and SUV (r=0.85, p=0.004) (**Figure 3**) was noted.

^{18}F-FDG: The correlation analysis revealed a significant linear correlation of r=0.90 with p<0.01 for SUV and time for Group C (**Figure 4**). All other correlations between the FDG quantitative parameters with time were not significant on the p<0.05 level for any group.

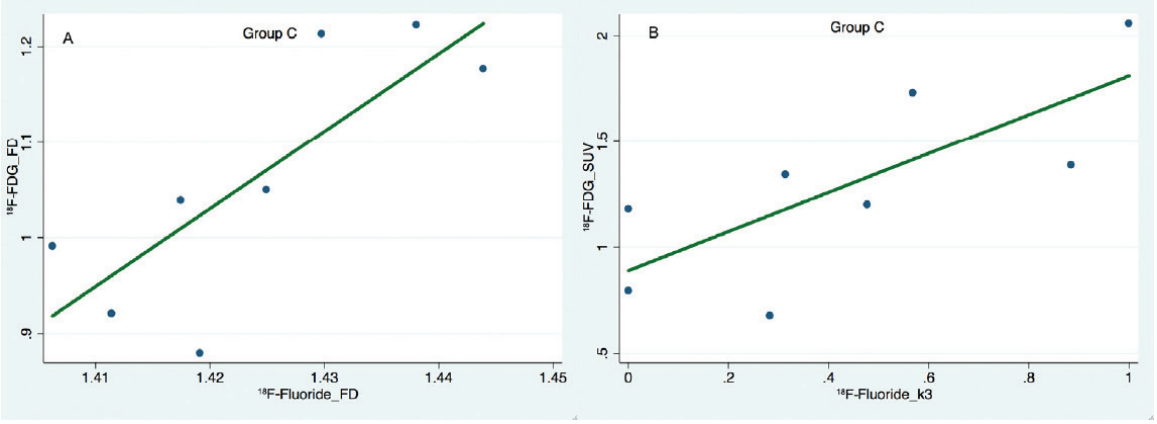

Figure 6. Scatter plots of dPET quantitative parameters from ^{18}F-Fluoride and ^{18}F-FDG in Group C. A significant correlation was obtained using a linear regression fit for (A) FD of ^{18}F-Fluoride and FD of ^{18}F-FDG (r=0.80, p<0.05), (B) k3 of ^{18}F-Fluoride and SUV of ^{18}F-FDG (r=0.75, p<0.05).

Comparison of tracers

We correlated the ^{18}F-Fluoride quantitative parameters with ^{18}F-FDG quantitative parameters. A negative significant correlation was only noted for K1 of ^{18}F-Fluoride and SUV of ^{18}F-FDG with r=-0.73 and p=0.04 (linear correlation) in Group K (**Figure 5A**). For Group D, the FD of ^{18}F-FDG was also significantly negative correlated with the FD of ^{18}F-Fluoride with r=-0.80 and p=0.02 (linear correlation) (**Figure 5B**). For Group C, significant positive correlations with $p<0.05$ were noted for FD of ^{18}F-FDG and FD of ^{18}F-Fluoride with r=0.80 (linear correlation) (**Figure 6A**), as well as for SUV of ^{18}F-FDG and k3 of ^{18}F-Fluoride with r=0.75 (linear correlation) (**Figure 6B**). The correlations of FD of ^{18}F-FDG and SUV of ^{18}F-Fluoride, SUV of ^{18}F-FDG and FD of ^{18}F-Fluoride were also significant on the $p<0.05$ level (data not shown).

Discussion

A widely used methodology to assess the osteoporotic changes is to measure the bone mineral density using Dual-energy X-ray absorptiometry (DEXA) measurements. DEXA scans were performed by another group of this multicenter project and revealed a reduction in bone mineral density 3 months after ovariectomy and start of either the vitamin D- and calcium-deficient diet (Group D) or the glucocorticoid treatment in the lumbar spine (Group C) as compared with the control group. In addition, T scores were well below -2.5 (-2.6 to –5.9) in both Group C and Group D, which further indicates pronounced osteoporotic status. Interestingly, the T score was significantly decreased in the Group D and less decreased in Group C [27].

Skeletal metabolic heterogeneities are of interest in the study of the pathophysiology of metabolic bone disorders including osteoporosis and also may help us to understand the different treatment responses observed with regard to bone mass and fracture risk at different skeletal sites [28-31]. In an experimental setting using molecular imaging modalities, like PET-CT in rats, the spine is the site of choice, in particular for quantitative assessment of bone metabolism. The reason is that the change in bone metabolism is greater than that observed at other skeletal sites; and the size and shape of the vertebral bodies make them amenable to accurate image analysis [32]. In this study, with the use of ^{18}F-fluoride and ^{18}F-FDG we have observed differences in regional skeletal kinetics of lumbar spine.

Since the publication by Hawkins et al. in 1992 reporting the feasibility of quantitatively assessing regional skeletal fluoride uptake in focal and generalized bone disease, the preferred tracer kinetic model is the 4k 3-compartmental model [12]. In addition, a comparison of quantification methods have been reported by Siddique [33]. In this study, 2-tissue compartment model (also known as a 3-compartment model) was used. The model is created based on simplification of physiological processes because of the heterogeneity of tissue within

PET VOI´s. For the input function, we used the aorta, which lies within the field of view and allows a noninvasive estimation. Furthermore, we calculated the fractal dimension (FD), which is a non-compartmental approach used to characterize the chaotic nature of the tracer's distribution in tissue, based on the box counting procedure of chaos theory. At our center, we routinely use this quantititative approaches for both patient and animal studies [19, 24, 26]. We preferred the use of the Biograph mCT 128S for the rat examinations instead of an animal scanner, because the system provides a high resolution over the whole field of view (1.9 mm in the center and 2.4 mm at the periphery of the 56 cm field of view). Furthermore, the CT provides a resolution of 150 μm. These systems properties allowed the simultaneous acquisition of two rats, which were placed in the center of the scanner. This fact reduced the acquisition time by 50%.

Radionuclide tracers such as ^{18}F-Fluoride binds to newly mineralizing bone, thus serving as a marker of bone blood flow and for osteoblastic activity [34]. The mechanism of uptake in bone is the deposition of fluoride ions in newly forming hydroxyapatite crystals at sites of bone formation, and hence the component of bone turnover being measured by $^{18}F^-$ imaging is osteoblastic activity. **Figure 1** demonstrated that fluoride has been shown to be preferentially deposited at bone surfaces where remodeling is greatest, and FDG shows the regional glucose metabolism of tissue.

The standardized uptake value (SUV) reflects the proportion of injected dose per milliliter of tissue taken up at a given time post-injection and is normalized to body weight. Herein bone turnover measured by SUV reflects the degree of osteoporosis.

For ^{18}F-Fluoride, rate constants K1 and k2 represent the fluoride ions exchange with hydroxyl groups of hydroxyapatite crystal of bone and the reverse process, respectively, whereas k3 and k4 represent the formation of fluoroapatite and the opposite respectively. VB reflects the amount of fractional blood volume in the VOI. Plasma clearance of fluoride to bone mineral (Ki) represents fluoride mass influx to the bone mineral compartment and has been shown to be correlated with histomorphometric indices including adjusted mineral apposition rate and bone formation rate as well as serum alkaline phosphatase and parathyroid hormone levels in renal osteodystrophy. In this study, k3 showed a significant increase with time in Group K for lumbar spine due to the increase the formation of fluoroapatite, reflecting the severity of the osteoporosis with time (as shown in **Figure 2A**). The results were similar for SUV and FD (**Figure 2B** and **2C**) in Group K. In addition, in Group D SUV revealed no significant correlation with time, but the increasing trend with time, which demonstrated a higher remodeling and glucose metabolism in lumbar spine (data were presented in supporting materials). A possible explanation is that, lumbar spine is a predominantly trabecular site, which is in keeping with greater turnover and bone formation, and reflects higher mineralization rates. Similarly, the parameter k2 in Group K decreased significantly with time (data not shown), indicating a lower rate of transfer from the bone extravascular compartment back to plasma and therefore enhancing the overall extraction efficiency from the extravascular compartment to bone mineral, which is associated with an increase in bone turnover. Cook et al. also found that k2 was significantly lower in pagetic bone [37]. However, the decrease in k2 was not associated with an increase in k3, which may be caused by a lack of statistical power or a greater degree of tissue heterogeneity than can be explained by a 2-tissue compartmental model.

Brenner et al. reported that the SUV of ^{18}F-fluoride PET correlated well with markers of bone metabolism [38]. We also gained similar results with an experimental rat model in Group C, which showed a significant correlation between Ki and SUV ($r=0.85$, $p=0.004$) (**Figure 3**). However, only K1 showed a significant decrease with time in Group C (glucocorticoid-induced osteoporosis). The significant decrease in K1 was accompanied by a non-significant decrease in Ki, although it has previously been shown that K1 and Ki are coupled under various physiological conditions [39-42]. This discordance can be explained by a non-significant decrease in the fraction of tracer in the extravascular tissue space that underwent specific binding to the bone matrix (k3/[k2+k3]). Other parameters showed inconsistent changes. Patients with glucocorticoid-induced osteoporosis have been reported to have abnormalities in global biochemical markers of bone turnover

and metabolism, which induced the inconsistent changes [43, 44]. Although in Group D (diet-induced osteoporosis) the parameters didn't show any significant correlation with time, they revealed consistent but not significant changes (increase) with time, including K1, k3, Ki and SUV, which reflects the increasing degree of osteoporosis with time.

Positron emission tomography using ^{18}F-FDG has been used to evaluate a variety of skeletal disorders. ^{18}F-FDG uptake is elevated in activated inflammatory cells such as leucocytes, granulocytes and macrophages because of increased glucose metabolism and expression of glucose transporters in these cells [45-47]. Bone healing involves an inflammatory phase, which represents a highly activated state of cell metabolism and glucose consumption, mimicking an infect on ^{18}F-FDG PET scanning [48, 49]. Furthermore, ^{18}F-FDG-PET is highly sensitive also in the detection of bone metastases. ^{18}F-FDG accumulation depends on the cellular uptake and phosphorylation of ^{18}F-FDG, which differs amongst various bones. For ^{18}F-FDG, the constants K1 and k2 are associated with the transport of non-metabolized ^{18}F-FDG into the cells, whereas k3 and k4 reflect the phosphorylation and dephosphorylation of the intracellular ^{18}F-FDG. Ca restriction in ovariectomized beagles was reported to induce the decrease in bone mass and strength and the increase in the bone turnover of the lumbar bone [50]. In Group C of this study, a positive significant correlation was also noted in SUV with time (**Figure 3**), which demonstrated an increasing glucose metabolism in lumbar spine of Group C with time. Osteoblastic cells, demonstrated by the formation of new bone could induce the increase of glucose transport and uptake, as reported before [35, 36]. But in Group D and Group K of this study, a non-significant decrease in bone turnover measured by SUV was found. In contrast to the ^{18}F-Fluoride data, parameters including K1, k3 and SUV of FDG showed consistent changes (increase) in Group C. Hsu et al. reported that PET scans using ^{18}F-FDG were not helpful in differentiating metabolic activity between normal and osteoporotic bones [51]. In this study, the change of other parameters except SUV in Group C from ^{18}F-FDG PET was inconsistent and didn't show any significant correlation with time too. The inconsistent results reported in the literature may reflect the fact that the changes in bone remodeling and glucose metabolism may be different for each osteoporosis type (e.g. juvenile vs. age-related osteoporosis). This is also true for our results including the two different osteoporosis induced models. We found significant differences only for the Group C, which is primarily hormone-dependent.

The correlation analysis of ^{18}F-Fluoride quantitative parameters with ^{18}F-FDG quantitative parameters revealed some significant linear correlations on the $p<0.05$ level. In Group K, we noted a significant correlation between the K1, which reflects the hydroxyl-exchange of fluoride and the global FDG uptake as reflected by the SUV. In the diet Group D, we found a significant but negative correlation between the FD of both tracers, which is indicative for a low heterogeneity of the time activity curve of each tracer. Different significant positive correlations were noted in Group C, e.g. between the FD of both tracers as well as between the k3 of 18F-Fluoride, which reflects the fixation of fluoroapatite and the global FDG uptake as measured in SUV.

Bone healing and therapeutic interventions can be monitored in animal experimental models, and dPET/CT, which is a well-established and validated qualitative and quantitative imaging tool. Our model of OVX-diet or OVX-steroid in rats may provide a useful model for age-depend bone loss in postmenopausal women, which has been indicated to be a multifactorial condition including estrogen deficiency and inadequate calcium intake [37, 52].

Conclusion

The study was designed to acquire a pronounced osteoporotic effect in rats by combining different strategies of osteoporosis induction and to understand the different mechanisms of steroid induced or nutrient deficiency on the osteoporotic bone. Time dependent significant differences in PET dynamic parameters were observed. The main results were an increase of certain kinetic parameters of ^{18}F-Fluoride in the lumbar spine with time and for all three groups, especially for Group K, which revealed a significant linear correlation. These sets of experiment will be further used by us for the long term study in a rat model followed by larger animal models ultimately leading to the future aim of development of new therapies for

osteoporosis, implants and bone materials for osteoporotic bone and fractures.

Acknowledgements

This study is part of the Sonderforschungsbereich-Transregio 79 (SFB-TR 79) and was financially supported by the Deutsche Forschungsgemeinschaft (German Research Foundation, DFG).

Conflict of interest

The authors declare that they have no conflict of interest.

Address correspondence to: Dr. Caixia Cheng, Clinical Cooperation Unit Nuclear Medicine, German Cancer Research Center, Im Neuenheimer Feld 280, D-69120 Heidelberg, Germany. Phone: 0049-6221-422501; Fax: 0049-6221-422476; E-mail: c.cheng@dkfz.de

References

[1] NIH Consensus Development Panel on Osteoporosis Prevention Diagnosis, and Therapy. Osteoporosis prevention, diagnosis, and therapy. JAMA 2001; 285: 785-795.

[2] Canto M, Prado C. The problem of osteoporosis and menopause in relation to morphophysiological characteristics. Int J Anthropol 1993; 8: 205-212.

[3] Dimai HP, Svedbom A, Fahrleitner-Pammer A, Pieber T, Resch H, Zwettler E, Chandran M, Borgström F. Epidemiology of hip fractures in Austria: evidence for a change in the secular trend. Osteoporos Int 2011; 22: 685-692.

[4] WHO. WHO scientific group on the assessment of osteoporosis at primary health care level. Summary Meeting Report. Brussels, Belgium, 5-7 May 2004.

[5] Kanis JA, Johnell O. Requirements for DXA for the management of osteoporosis in Europe. Osteoporos Int 2005; 16: 229-238.

[6] Cummings SR, Bates D, Black DM. Clinical use of bone densitometry: scientific reviews. JAMA 2002; 288: 1889-1897.

[7] Unnanuntana A, Gladnick BP, Donnelly E, Lane JM. The assessment of fracture risk. J Bone Joint Surg Am 2010; 92: 743-753.

[8] Zebaze RM, Ghasem-Zadeh A, Bohte A, Iuliano-Burns S, Mirams M, Ian Price R, Mackie JE, Seeman E. Intracortical remodeling and porosity in the distal radius and post-mortem femurs of women: a cross-sectional study. Lancet 2010; 375: 1729-1736.

[9] Fogelman I, Cook G, Israel O, van der Wall H. Positron emission tomography and bone metastases. Semin Nucl Med 2005; 35: 135-142.

[10] Grant FD, Fahey FH, Packard AB, Davis RT, Alavi A, Treves ST. Skeletal PET with 18F-Fluoride applying new technology to an old tracer. J Nucl Med 2008; 49: 68-78.

[11] Schmitz A, Risse JH, Textor J, Zander D, Biersack HJ, Schmitt O, Palmedo H. FDG-PET findings of vertebral compression fractures in osteoporosis: preliminary results. Osteoporos Int 2002; 13: 755-761.

[12] Hawkins RA, Chio Y, Huang SC, Hoh CK, Dahlbom M, Schiepers C, Satyamurthy N, Barrio JR, Phelps ME. Evaluation of skeletal kinetics of fluoride ion with PET. J Nucl Med 1992; 33: 633-642.

[13] Blau M, Ganatra R, Bender M. 18F-fluoride for bone imaging. Semin Nucl Med 1972; 2: 31-37.

[14] Narita N, Kato K, Nakagaki H, Ohno N, Kameyama Y, Weatherell JA. Distribution of fluoride concentration in rat bone. Calcif Tissue Int 1990; 46: 200-204.

[15] Ishiguro K, Nakagaki H, Tsuboi S, Narita N, Kato K, Li J, Kamei H, Yoshioka I, Miyauchi K, Hosoe H, Shimano R, Weatherell JA, Robinson C. Distribution of fluoride in cortical bone of human rib. Calcif Tissue Int 1993; 52: 278-282.

[16] Reeve J, Arlot M, Wootton R, Edouard C, Tellez M, Hesp R, Green JR, Meunier PJ. Skeletal blood flow, iliac histomorphometry and strontium kinetics in osterporosis: A relationship between blood flow and corrected apposition rate. J Clin Endocrinol Metab 1988; 66: 1124-1131.

[17] Toorongian SA, Mulholland GK, Jewett DM, Bachelor MA, Kilbourn MR. Routine production of 2-deoxy-2 (^{18}F)fluoro-$_D$-glucose by direct nucleophilic exchange on a quaternary 4-aminopyridinium resin. Nucl Med Biol 1990; 3: 273-279.

[18] Satyamurthy N, Amarasekera B, Alvord CW, Barrio JR, Phelps ME. Tantalum [^{18}O]water target for the production of [^{18}F]fluoride with high reactivity for the preparation of 2-deoxy-2-[18F]fluoro-D-glucose. Mol Imaging Biol 2002; 4: 65-70.

[19] Strauss LG, Conti PS. The applications of PET in clinical oncology. J Nucl Med 1991; 32: 623-648.

[20] Mikolajczyk K, Szabatin M, Rudnicki P, Grodzki M, Burger C. A JAVA environment for medical image data analysis: initial application for brain PET quantitation. Med Inform 1998; 23: 207-214.

[21] Burger C, Buck A. Requirements and implementations of a flexible kinetic modelling tool. J Nucl Med 1997; 38: 181-1823.
[22] Miyazawa H, Osmont A, Petit-Taboue MC, Tillet I, Travera JM, Zoung AR, Barre L, MacKenzie ET, Baron JC. Determination of 18F-Fluoro-2-deoxy-D-glucose rte constants in the anesthetized baboon brain with dynamic positron tomography. J Neurosci Methods 1993; 50: 263-272.
[23] Sokoloff L, Smith CB. Basic principles underlying radioisotopic methods for assay of biochemical processes in vivo. In: Greitz T, Ingvar DH, Widén L, eds. The Metabolism of the Human Brain Studies with Positron Emission Tomography. New York, NY: Raven Press; 1983; 123-148.
[24] Cheng C, Alt V, Dimitrakopoulou-Strauss A, Pan L, Thormann U, Schnettler R, Weber K, Strauss LG. Evaluation of New Bone Formation in Normal and Osteoporotic Rats with a 3-mm Femur Defect: Functional Assessment with Dynamic PET-CT (dPET-CT) Using a 2-Deoxy-2-[^{18}F]Fluoro-D-glucose (^{18}F-FDG) and ^{18}F-Fluoride. Mol Imaging Biol 2012; In Print.
[25] Strauss LG, Pan L, Koczan D, Klippel S, Mikolajczyk K, Burger C, Haberkorn U, Schonleben K, Thiesen HJ, Dimitrakopoulou-Strauss A. Fusion of positron emission tomography (PET) and gene array data: a new approach for the correlative analysis of molecular biological and clinical data. IEEE Trans Med Imaging 2007; 26: 804-12.
[26] Dimitrakopoulou-Strauss A, Strauss LG, Burger C, Mikolajczyk K, Lehnert T, Bernd L, Ewerbeck V. On the fractal nature of dynamic positron emission tomography (PET) studies. World J Nucl Med 2003; 2: 306-313.
[27] Heiss C, Govindarajan P, Schlewitz G, Hemdan N, Schliefke N, Alt V, Thormann U, Lips KS, Wenisch S, Langheinrich AC, Zahner D, Schnettler R. Induction of osteoporosis with its influence on osteoporotic determinants and their interrelationships in rats by DEXA. Med Sci Monit 2012; 18: BR199-207.
[28] Duan Y, Tabensky A, Deluca V, Seeman E. The benefit of hormone replacement therapy on bone mass is greater at the vertebral body than posterior processes or proximal femur. Bone 1997; 21: 447-451.
[29] Bell KI, Loveridge N, Power J, Garrahan N, Stanton M, Lunt M, Meggitt BF, Reeve J. Structure of the femoral neck in hip fracture: Cortical bone loss in the inferoanterior to superoposterior axis. J Bone Miner Res 1994; 14: 111-119.
[30] Yoshida Y, Moriya A, Kitamura K, Inazu M, Okimoto N, Okazaki Y, Nakamura T. Responses of trabecular and cortical bone turnover and bone mass and strength to bisphosphonate YH529 in ovariohysterectomized beagles with calcium restriction. J bone Miner Res 1998; 13: 1011-1022.
[31] Israel O, Lubushitzky R, Frenkel A, Iosilevsky G, Bettman L, Gips S, Hardoff R, Baron E, Barzilai D, Kolodny GM. Bone turnover in cortical and trabecular bone in normal women and women with osteoporosis. J Nucl Med 1994; 35: 1155-1158.
[32] Blake GM, Fogelman I. Interpretation of bone densitometry studies. Semin Nucl Med 1997; 27: 248-260.
[33] Siddique M, Frost ML, Blake GM, Moore AEB, Al-Beyatti Y, Marsden PK, Schleyer PJ, Fogelman I. The precision and sensitivity of ^{18}F-Fluoride PET for measuring regional bone metabolism: a comparison of quantification methods. J Nucl Med 2011; 52: 1748-1755.
[34] Reeve J, Arlot M, Wootton R, Edouard C, Telley M, Hesp R, Green JR, Meunier PJ. Skeletal blood flow, iliac histomorphometry, and strontium kinetics in osteoporosis: a relationship between blood flow and corrected apposition rate. J Clin Endocrinol Metab 1998; 66: 1124-1131.
[35] Zoidis E, Ghirlanda-keller C, Schmid C. Stimulation of glucose transport in osteoblastic cells by parathyroid hormone and insulin-like growth factor I. Mol Cell Biochem 2011; 348: 33-42.
[36] Zoidis E, Ghirlanda-Keller C, Schmid C. Thriodothyronine stimulated glucose transport in bone cells. Endocrine 2012; 41: 501-11.
[37] Cook GJR, Blake GM, Marsden PK, Cronin B, Fogelman I. Quantification of skeletal kinetic indices in paget's disease using dynamic ^{18}F-fluoride positron emission tomography. J Bone Miner Res 2002; 17: 854-859.
[38] Brenner W, Vernon C, Muzi M, Mankoff DA, Link JM, Conrad EU, Eary JF. Comparison of different quantitative approaches to 18F-fluoride PET scans. J Nucl Med 2004; 45: 1493-1500.
[39] Piert M, Zittel TT, Becker GA, Jahn M, Stahlschmidt A, Maier G, Machulla H-J, Bares R. Assessment of porcine bone metabolism by dynamic ^{18}F-fluoride PET: correlation with bone histomorphometry. J Nucl Med 2001; 42: 1091-1100.
[40] Messa C, Goodman WG, Hoh CK, Choi Y, Nissenson AR, Salusky IB, Phelps ME, Hawkins RA. Bone metabolic activity measured with positron emission tomography and ^{18}F-fluoride ion in renal osteodystophy: correlation with bone histomorphometry. J Clin Endocrinol Metab 1993; 77: 949-955.
[41] Berding G, Burchert W, van den Hoff J, Pytlik C, Neukam FW, Meyer GJ, Gratz KF, Hundeshagen

H. Evaluation of the incorportation of bone grafts used in maxillofacial surgery with ^{18}F-fluoride ion and dynamic positron emission tomography. Eur J Nucl Med 1995; 22: 1133-1140.

[42] Piert M, Machulla H-J, Jahn M, Stahlschmidt A, Becker GA, Zittel TT. Coupling of porcine bone blood flow and metabolism in high-turnover bone disease measured by $^{15}OH_2O$ and ^{18}F-fluoride ion positron emission tomography. Eur J Nucl Med Mol imaging 2002; 29: 907-914.

[43] Conti A, Sartorio A, Ferrero S, Ferrario S, Ambrosi B. Modification of biochemical markers of bone and collagen turnover during corticosteroid therpy. J Endocrinol Invest 1996; 19: 127-130.

[44] Kollerup G, Hansen M, Horslev-Petersen K. Urinary hydrooxypyridinium crosslinks of collagen in rheumatoid arthritis: ralation to disease activity and effects methyprednisolone. Br J Rheumatol 1994; 33: 816-820.

[45] Stumpe KD, Dazzi H, Schaffner A, von Schulthess GK. Infection imaging using whole-body FDG-PET. Eur J Nucl Med 2000; 27: 822-832.

[46] Schulte M, Brecht-Krauss D, Heymer B, Guhlmann A, Hartwig E, Sarkar MR, Diederichs CG, Von Bär A, Kotzerke J, Reske SN. Grading of tumors and tumorlike lesion of bone: evaluation by FDG PET. J Nucl Med 2000; 41: 1695-1701.

[47] Aoki J, Watanabe H, Shinozaki T, Takagishi K, Ishijima H, Oya N, Sato N, Inoue T, Endo K. FDG PET of primary benigh and malignant bone tumors: standardized uptake value in 52 lesions. Radiology 2001; 219: 774-777.

[48] de Winter F, Vogelaers D, Gemmel F, Dierckx RA. Promising role of 18-F-fluoro-D-deoxyglucose positron emission tomography in clinical infectious diseases. Eur J Clin Microbiol Infect Dis 2002; 21: 247-257.

[49] Koort JK, Mäkinen TJ, Knuuti J, Jalava J, Aro HT. Comparative 18F-FDG-PET imaging of experimental *staphylococcusaureus* osteomyelitis and normal bone healing. J Nucl Med 2004; 45: 1406-1411.

[50] Yoshida Y, Moriya A, Kitamura K, Inazu M, Okimoto N, Okazaki Y, Nakamura T. Responses of trabecular and cortical bone turnover and bone mass and strength to bisphosphonate YH529 in ovariohysterectomized beagles with calcium restriction. J bone Miner Res 1998; 13: 1011-1022.

[51] Hsu WK, Feeley BT, Krenek L, Stout B, Chatziioannou AF, Lieberman JR. The use of 18F-fluoride and 18F-FDG PET scans to assess fracture healing in a rat femur model. Eur J Nucl Mol Imaging 2007; 34: 1291-1301.

[52] Uchida K, Nakajima H, Miyazaki T, Yayama T, Kawahara H, Kobayashi S, Tsuchida T, Okazawa H, Fujibayashi Y, Baba H. Effects of alendronate on bone metabolism in glucocorticoid-induced osteoporosis measured by ^{18}F-Fluoride PET: a prospective study. J Nucl Med 2009; 50: 1808-1814.

Supporting materials

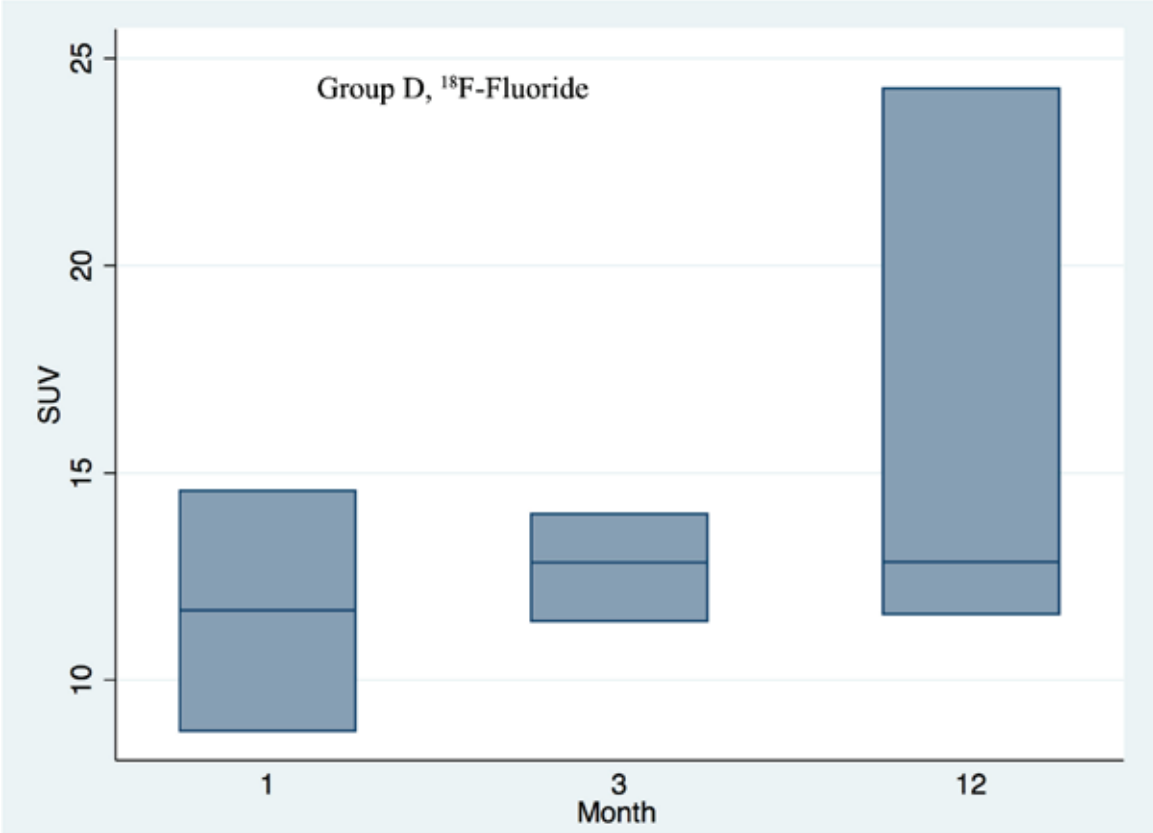

SUV revealed the increasing trend with time in Group D.